



Yield displacement charts for performance-based seismic design

Enrique Hernández-Montes¹  · María L. Jalón¹ · Juan Chiachío¹ ·
Luisa María Gil-Martín¹

Received: 10 March 2022 / Accepted: 4 October 2022
© The Author(s) 2022

Abstract

A new tool for seismic design is presented, called Yield Displacement Charts (YDC). As with its predecessors, the Yield Point Spectra (YPS) and the Yield Frequency Spectra (YFS), the YDC concept takes advantage of the simple features of yield displacement (u_y), to use u_y in a performance-based design instead of a force-based period-dependent approach. A self-contained and comprehensive approach to YPS and YFS is presented, enabling the novel aspect of YDC to be introduced: a tool for a multi-performance objective design that only depends on the location of the structure to be designed. Once the yield displacement chart has been calculated for a particular place, it can be used for the preliminary design of any structure. For a given value of yield displacement, the YFS are obtained from the Yield Displacement Chart. The suitability of the methodology proposed is illustrated by means of a simple case study of a concrete bridge pier.

Keywords Performance-based design · Yield displacement · Yield frequency spectra · Preliminary design

1 Introduction

The seismic design process always needs to start with a preliminary design (Aschheim et al. 2019; Palermo et al. 2016). The accuracy of the preliminary design is of paramount importance, since if the final design is similar to the preliminary one, numerous redesign cycles can be avoided. The stiffness of a structure (or equivalently, its natural period) is related to its seismic demand. As structural displacements caused by earthquakes primarily follow the shape of the first mode of vibration, preliminary seismic designs are generally based on the response of single-degree-of-freedom systems (Aschheim et al. 2019). These are characterized by their natural period in the elastic range. Approximate expressions of the natural period of the most common structures are available in the literature and in professional codes. Starting an iteration process

✉ Enrique Hernández-Montes
emontes@ugr.es

¹ School of Civil Engineering, University of Granada, Granada, Spain

between seismic demand and natural period up to convergence (Chopra and Goel 2001) only requires an initial estimation of the value of the natural period.

For design purposes, the natural period can be used in force-based design (e.g. EN1998-1 2004) or in performance-based design (Deierlein 2004). The fundamentals of performance-based design, outlined in the Vision 2000 report (SEAOC 1995), are now widely accepted.

In addition to the natural period, yield displacement (u_y) has proven to be a stable and useful parameter for performance-based design, (Priestley 2000; Aschheim 2002). In this article, yield displacement is used as a primary structural parameter to obtain a first value of the seismic demand of a structure. The objective of this article is to determine the seismic demand for various performance objectives. This will be carried out using Yield Displacement Charts (YDC). The great advantage of YDC is that they only depend on the location of a structure.

The first section of the article is dedicated to describing, in a mathematically compact and simple way, the response of a single degree-of-freedom system in the linear elastic domain and in the plastic domain. The second section presents the seismic hazard curve (peak ground acceleration -PGA- versus probability of occurrence), particularized for Granada -Spain-. For preliminary design, the intensity of ground motion is expressed in terms of the PGA, although it implies conservatism. PGA can be substituted by period-dependent (e.g. the spectral acceleration, $S_a(T)$, (Luco and Bazzurro 2007)) or non-period-dependent descriptors (e.g. peak ground velocity (Palermo et al. 2014)).

Several spectral representations of the seismic demand of single degree-of-freedom (SDOF) systems are available in the literature, (Chopra 2020). The most common representation is pseudo-acceleration versus the period of the SDOF system. However, yield point spectra (YPS) uses yield displacement (u_y) as an alternative to the period (T) (Mark Aschheim and Black 2000). The great advantage of yield displacement is that, for a given structural configuration, it is a more stable parameter than the elastic period, which is a useful property in preliminary designs. The properties of yield displacement are explained in the third section of this paper.

In the fourth section, the YDC are created. YDC are represented in a reference system whose axes are yield displacement, ductility demand and mean annual frequency. Given its suitability for design purposes, yield displacement has been used instead of the elastic period (Aschheim et al. 2019). Moreover, although it has not been adequately substantiated, the elastic period has not been used with in the article to emphasize the fact that the elastic period loses part of its physical meaning in the plastic range.

Performance-based seismic designs that consider several performance objectives corresponding to different seismic hazard levels are now more commonly used, and they are recommended in (SEAOC 1999 and FIB 2012). In this context, Yield Frequency Spectra (YFS) (Vamvatsikos and Aschheim 2016) are considered to be efficient tools for dealing with this type of analysis. YFS are graphical representations that link the mean annual frequency/rate (MAF) of ductility threshold being exceeded (i.e. a performance objective) to the system yield strength coefficient (C_y). YFS are plotted for a given yield displacement (u_y), and they enable the system demand for different performance objectives to be visualized. The fifth section deduces the YFS from the theoretical framework of conditional probability, and YDC are presented. Like the YFS, the YDC are graphical representations of the system demand for given performance objectives, but unlike YFS, YDC are obtained by considering yield displacement as a variable, so the result is a performance-based seismic design tool that only depends on the geographical location of the structure.

YDC can be considered as the latest member of the family of Yield Displacement Based Design Spectra: Yield Point Spectra (YPS), Yield Frequency Spectra (YFS), and Yield Displacement Charts (YDC). YPS are used for deterministic analysis while YFS and YDC are meant for probabilistic approaches. Given that u_y is a new variable in the definition of YDC, a spectrum that only depends on the location of a structure is obtained. This factor could make them the most attractive member of the family. Finally, in the fifth section the yield displacement chart for the City of Granada is calculated, and a simple example of structural design is developed.

2 The response of the single degree-of-freedom system

The time-history displacement response, $u(t)$, of a linear-elastic SDOF system, for a fixed value of damping, subjected to a given ground motion, $\ddot{u}_g(t)$, is characterized by only one variable, which is usually the elastic period T . From this period, $\omega = 2\pi/T$ and $k = \omega^2 m$ can be computed, with k as the initial stiffness, m the mass and ω the natural circular frequency of the system (see Fig. 1). The maximum displacement of a linear-elastic SDOF for a given ground motion is called elastic spectral displacement $S_d = \max[u(t)]$, for which the SDOF develops an elastic force $F_e = k S_d$. Typically, this elastic force is presented in the literature as being divided by mass m , and, in this case, it is called *spectral pseudo-acceleration*: $S_a = F_e/m$. By using the simple relationships above, it can be demonstrated that $S_a = \omega^2 S_d$. Since T characterizes the SDOF response for a given ground motion, all the variables defined above can be expressed as functions of T , i.e.: $S_a(T)$, $S_d(T)$ and $F_e(T)$. For example, the (pseudo-acceleration) response spectrum of a ground motion can be represented by $S_a(T)$ versus T , as shown in Fig. 2.

In structural engineering design, seismic action is not unique (note that Fig. 2 corresponds to a specific seismic accelerogram, $\ddot{u}_g(t)$). Thus, a probabilistic treatment of seismic action is required. Simple envelope approximations of uniform-hazard response spectra derived from probabilistic seismic hazard analysis (PSHA, Cornell 1968) are used in professional standards (i.e. ASCE7 2022, EN1998-1) for structural design purposes: the *design spectra*. For a SDOF system of period T and mass m , the design spectrum gives the maximum elastic force that can be developed by the SDOF system, $S_a(T)m$, for a certain probability of occurrence, e.g. 10% in 50 years.

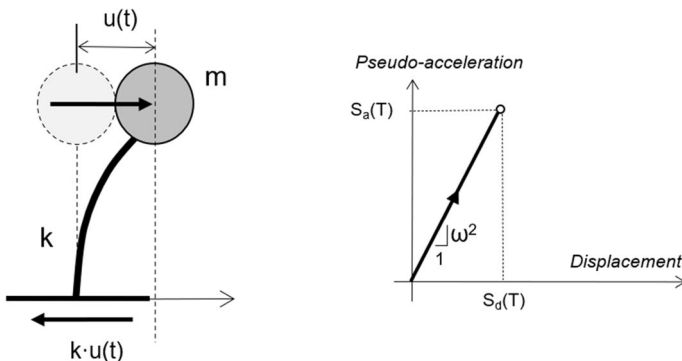


Fig. 1 Characterization of the linear elastic SDOF and its response

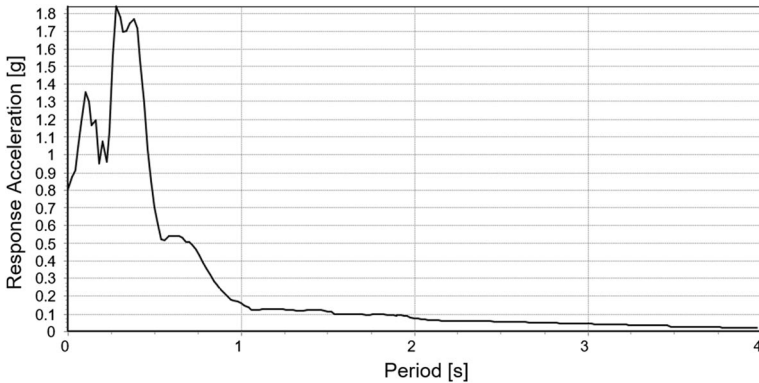


Fig. 2 Pseudo-acceleration response spectra for the *Corralitos* record of the Loma Prieta Earthquake in October 17, 1989, for 5% damping

Likewise, a non-linear SDOF system modeled as elasto-plastic can be characterized by only two variables, usually C_y and u_y , with u_y being the yield displacement and C_y being the yield strength coefficient, defined as $C_y = F_y/mg$ where F_y is the yield strength (see Fig. 3). Note the apparent absence of the elastic period in this characterization, which is defined via C_y and u_y as

$$T = 2\pi \sqrt{\frac{u_y}{C_y g}} \tag{1}$$

If for a given ground motion, the maximum displacement of this non-linear system, is u_{max} so that if $u_{max} > u_y$, then the maximum displacement is within the plastic range. It is important to note that once the system is on the yield plateau, the main recovery factor of the system in terms of displacement is the cyclical nature of the seismic action itself, whereby the system alternates between unloading/reloading at elastic stiffness (or near-elastic for non-kinematic-hardening hysteresis rules), and it sustains further damage along the yield plateau. In other words, the importance of a period as a performance-prediction variable is limited when the system enters the post-yield range. The reader should be aware that the

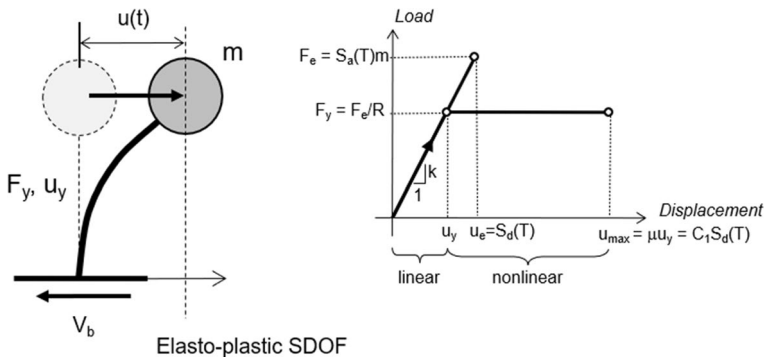


Fig. 3 Characterization of the elasto-plastic SDOF and its response

authors are looking for a simple preliminary design tool, not a complete and comprehensive description of the response.

In the time-history analysis, ductility (μ) is defined as u_{\max}/u_y (i.e., ductility demand). Given that demand D should not exceed capacity C (i.e. $D < C$), it is necessary to ensure that the ductility demanded by the earthquake is lower than the ductility capacity of the structure. In other words, when designing for a certain level of ductility, the designer needs to ensure that the structure is going to allow reliable plastic behavior in the areas of (pre-designated) structural detailing where plasticity is going to occur (i.e., ductility capacity). For the sake of mathematical completeness, values of μ that are lower than 1 are going to be considered (even if they are not proper ductility) in order to also include the cases where u_{\max} is lower than u_y in the study, which refers to the cases where displacement demand does not exceed the yield displacement of the structure. Even though the SDOF can be characterized by one or two variables, depending on whether it is linear or elasto-plastic, the (maximum or worst-case) response of the system can be described by only one variable: the maximum displacement, S_d or u_{\max} . The inelastic displacement ratio C_1 is defined to relate $S_d(T)$ and u_{\max} , so that $u_{\max} = C_1 S_d(T)$, FEMA 440 (FEMA 2005).

A simple way to describe the intensity of a ground motion is S_d , because it shows, as no other parameter does, the effect of a specific ground motion on an elastic SDOF of period T . Note that, as previously mentioned, $S_a = \omega^2 S_d$, lending the same properties of S_d to S_a . As previously discussed, the strength of this relationship is weakened when it enters the non-linear range. This is quantified by the use of inelastic displacement ratios $C_1(C_y, T)$, also known as R - μ - T strength ratio/ductility/period relationships (where R is essentially C_y , see Fig. 3), (Veletsos and Newmark 1960; Miranda and Bertero 1994; Ruiz-García and Miranda 2003). Since the connection is no longer deterministic, these relationships convey the statistics of inelastic displacement u_{\max} for systems of a given C_y and T , typically offering the mean estimate, $\overline{u_{\max}}$, for use in tandem with the static pushover (FEMA 2005; EN1998-3 2005):

$$\overline{u_{\max}} = C_{1m}(C_y, T) S_d(T) \tag{2}$$

where C_{1m} is the mean inelastic displacement ratio function for a given C_y and T .

The predictive ability of S_d and S_a , as intensity measures (IMs) within the framework of Performance-Based Earthquake Engineering (Cornell and Krawinkler 2000), can be characterized by implementing the associated dispersion of the distribution of $C_1(C_y, T)$, as offered by (Vamvatsikos and Cornell 2006) or (Ruiz-García and Miranda 2007). This is known as IM efficiency (Luco and Cornell 2007), and the lower the dispersion, the higher the efficiency and associated predictive capability. The issue of IM sufficiency also arises (Nicolas Luco and Cornell 2007). This characterizes the capability of S_d and S_a to render the distribution of $C_1(C_y, T)$, or, equivalently, of u_{\max} conditioned on S_d or S_a , which are independent of other seismological characteristics.

Sufficiency is a particularly useful property, as it negates (or generally reduces) bias when assessing performance (see Sect. 4). $S_d(T)$ is moderately efficient and sufficient, but clearly imperfect whenever large excursions into non-linearity or significantly higher-mode effects are involved (Luco and Bazzurro 2007). At the same time, $S_a(T)$ is clearly better than peak ground acceleration PGA (Kazantzi and Vamvatsikos 2015) for everything but the shortest periods, in which both parameters are practically identical. Despite everything described above, in the YDC presented, the authors are going to use PGA as the intensity measure, emphasizing the fact that it is not period dependent, which makes it more versatile than $S_d(T)$ even though it reduces efficiency and sufficiency. The authors believe

this tradeoff is acceptable for practical design applications, where simplicity is important, and conservativeness can be added as needed to make up for the probabilistic deficiencies of *PGA*. Definitely, new IMs containing elastic and plastic structural properties should be investigated to improve sufficiency and efficiency.

3 Seismic hazard

The intensity of ground motion at a certain site can be measured by IMs that, among other parameters, can be represented, as mentioned, by peak ground acceleration *PGA* or pseudo-acceleration $S_a(T)$. The level of ground motion intensity expected at a site is associated with a certain frequency/rate of occurrence, and this is calculated by using the total probability theorem, combining several probabilistic distributions, and conveying information about the seismic sources (faults), the site (e.g., soil type), and the source-to-site propagation (Baker 2013). This is known as probabilistic seismic hazard analysis (PSHA), and a representation of the intensity of ground motion, measured by the *PGA* versus its MAF is the seismic hazard curve $\lambda(PGA)$.

In this study, YDC was built for the city of Granada (latitude 37.18°, longitude -3.60°) using the site-specific hazard curve, $\lambda(PGA)$, using the seismic source model (Giardini et al. 2014) as estimated by (EFEHR 2021), considering a soil with an average shear wave speed in the upper 30 m of $V_{s30} = 250$ m/s. The seismic hazard curve is approximated by using a continuous smooth interpolation curve (splines), as shown in Fig. 4.

4 The use of yield displacement for seismic design

A preliminary design can be made based on the displacement response corresponding to the first mode of the structure, or to a combination of some of the modes, which is known as the equivalent single degree-of-freedom (ESDOF) system (Aschheim et al. 2019).

As an alternative, some displacement-based methods for seismic design (Mark Aschheim and Black 2000; Paulay 2002) use an estimation of yield displacement for establishing values of base shear strength. The main advantage of yield displacement, instead of the period, is that it is very stable when there are changes in the stiffness of a structure. This stability has been confirmed both at sectional and global system levels (Hernández-Montes and Aschheim 2003; Priestley et al. 2007; Hernández-Montes et al. 2019). As an

Fig. 4 Seismic hazard curve (black dots) and the fitting model (red line). Granada (Spain), $V_{s30} = 250$ m/s

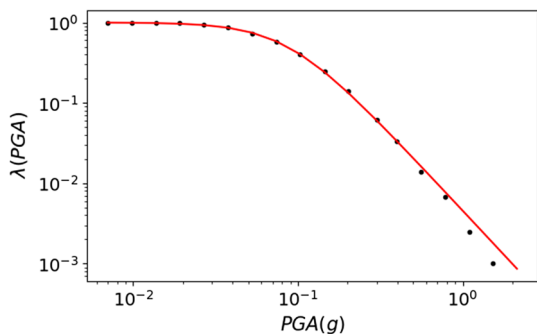


illustration of this feature, Fig. 5 shows the base shear resultant of two buildings subjected to a monotonic lateral force as a function of the roof displacement. The only difference between the two models in Fig. 5 is the amount of reinforcement. Figure 5 shows that the yield displacement (u_y) remains stable (gray bar in Fig. 5).

So, the stability of yield displacement converts it into a key performance variable for the seismic design of structures (Aschheim and Montes 2003). Estimations of yield displacement for several structural systems and different cross-sections can be found in Chapter 9 of (Aschheim et al. 2019).

5 Yield displacement charts

The performance of a SDOF system under a seismic action, formulated in terms of conditional probability, can be described as the MAF (λ) by which the maximum displacement (u_{max}) exceeds a certain limit displacement (δ):

$$\lambda(\delta|C_y, u_y) = P[u_{max} > \delta|C_y, u_y] = \int_0^\infty P[u_{max} > \delta|PGA, C_y, u_y] d\lambda(PGA) \quad (3)$$

where $\lambda(\bullet)$ denotes the MAF of its argument, $P[u_{max} > \delta|PGA, C_y, u_y]$ is the probability of u_{max} exceeding a threshold of δ conditioned by the yield strength coefficient (C_y), yield displacement (u_y), and on peak ground acceleration (PGA). The second term inside the integral is the differential of the PGA seismic hazard curve. Note that, by assuming the sufficiency of the IM (here PGA), any conditioning on seismological characteristics such as magnitude or distance has been dropped, at least in this term. This is a key assumption of the conditional approach (Bazzurro et al. 1998) that allows this standard treatment of Performance-Based Earthquake Engineering.

The integral above can be solved numerically as:

$$\lambda(\delta|C_y, u_y) = \sum_{j=1}^N P[u_{max} > \delta|PGA_j, C_y, u_y] \Delta\lambda(PGA_j) \quad (4)$$

where $\Delta\lambda(PGA_j) = \lambda(PGA_j) - \lambda(PGA_{j+1})$, with $PGA_{j+1} > PGA_j$.

Since the integral (or summation) is calculated over the IM , here, with the IM as PGA , the variable PGA disappears when the integral is completed. For a particular system, given by C_y and u_y , the above equation can be represented as a curve of $\lambda-\delta$, see Fig. 6a. It can be observed that when displacement threshold values (δ) increase, the probability that

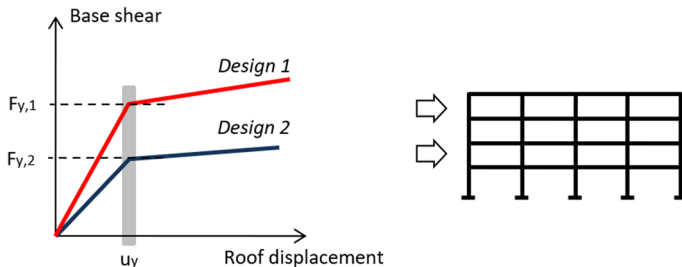


Fig. 5 Yield displacement of two models that differ only in component reinforcement quantity

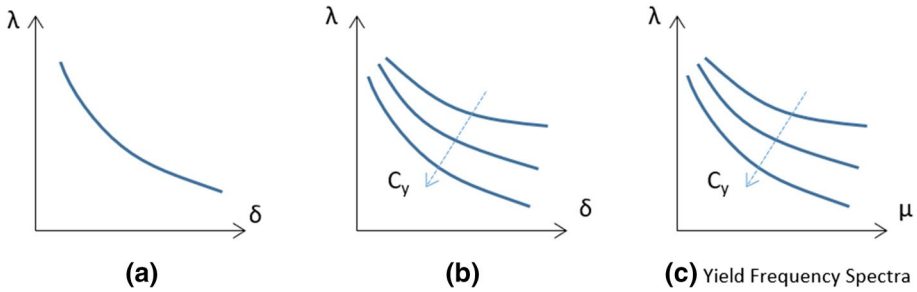


Fig. 6 Development of the yield frequency spectra

u_{max} exceeds δ decreases, see Fig. 6a. Additionally, C_y can be considered to be a variable. Curves of a constant value of C_y can be plotted together as in Fig. 6b. It can be observed that as the value of C_y increases, the probability of exceedance decreases.

The limit displacement (δ) divided by u_y is the ductility threshold, μ (i.e. $\mu = \delta/u_y$). So, if the horizontal axis of Fig. 6b is changed from δ to μ (see Fig. 6c) the Yield Frequency Spectra (YFS) is obtained (Vamvatsikos and Aschheim 2016).

As shown in Fig. 6c, for an elasto-plastic SDOF system whose yield displacement (u_y) is known, the YFS relates the probability of the exceedance of a given displacement threshold at a certain place (where the seismic hazard and the soil characteristics are known). Therefore, YFS are created for a specific location and for a constant value of u_y .

As previously mentioned, the yield displacement, u_y , is very stable when there are stiffness changes, which makes YFS the perfect tool for starting a multi-objective design. A new design tool arises if u_y is considered as a variable: The Yield Displacement Charts, see Fig. 7. The variables of the YDC are yield displacement (u_y) and the ductility threshold (μ) from which the yield strength coefficients (C_y) are obtained. Yield Displacement Charts are functions created in an ad hoc manner for a specific location.

For a series of values of C_y and u_y within a feasible range, the resulting curves, λ - δ , provide charts that are only dependent on the location of the structure, i.e., the charts are independent of the characteristics of the system. In the next step of design, for the value of u_y corresponding to a particular structural system (Chapter 9 of (Aschheim

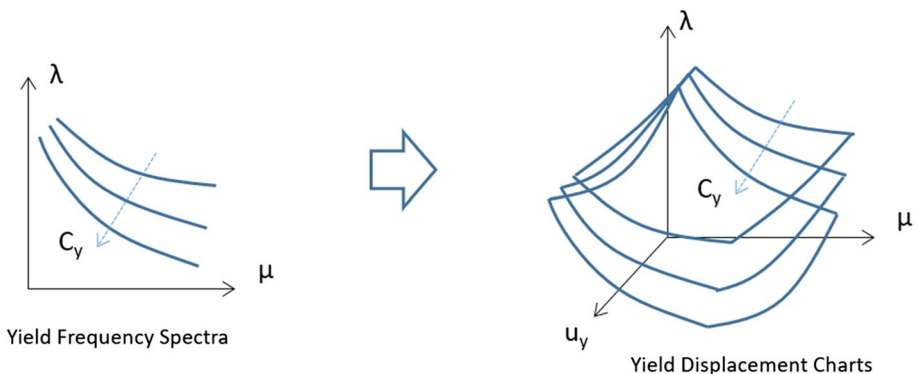


Fig. 7 Yield displacement charts

et al. 2019)), a YFS is obtained from the yield displacement chart. By using the YFS, the base shear for different performance objectives can be obtained (Vamvatsikos and Aschheim 2016).

The values of u_y , approximations are available in the literature for different types of structures (Aschheim, Hernández-Montes and Vamvatsikos 2019). Furthermore, the maximum displacements permitted are given by codes, so once the yield displacement is known, these limitations can be expressed as ductility limitations. Consequently, YDC are represented in terms of ductility and yield displacement.

6 Implementation of yield displacement charts

For a large set of elastic-hardening bilinear SDOF systems defined by C_y and u_y (see Fig. 8), the maximum displacement values u_{max} are obtained by using a database of 980 earthquakes. For all the SDOFs, as in (Heresi et al. 2018), 5% damping and 3% of post-yield stiffness ratio ($\gamma=0.03$, see Fig. 8) are considered. Additionally, a degraded elastic stiffness is used (k_u), defined as:

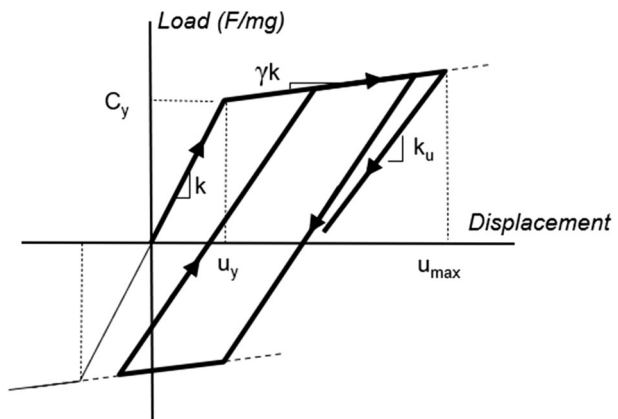
$$k_u = k \left(\frac{u_y}{u_{max}} \right)^\alpha \tag{5}$$

For reinforced concrete structures α ranges from 0.0 to 0.5. In this study $\alpha=0.5$ is used (Nielsen and Imbeault 1970).

All the ground motions used in this study have been obtained from (RESORCE 2020). No additional corrections were applied to the downloaded ground motion records. The filtering parameters applied in the process of record selection are as follows:

- Records with a moment magnitude (M_W) greater than 5 are selected (Aschheim, Hernández-Montes and Vamvatsikos 2019).
- Any source-to-site distance
- Both pulse-like and non-pulse-like motions
- Records with V_{S30} between 180 and 360 m/s.

Fig. 8 Elastic-hardening bilinear model with stiffness degradation



- Both of the horizontal component recordings available are considered.

As a sample, Fig. 9 shows, for the case of $C_y=0.3$ and $u_y=0.025$ m, the u_{max} obtained for the set of 980 ground motions considered (a dataset of 490 ground motions with two components each). A high dispersion is observed for $PGA > 0.2$ g, where high structural nonlinearity appears, which few records have. Specifically, there are 952 motions in $0 < PGA \leq 0.2$ g whereas there are only 28 motions in $0.2 \text{ g} < PGA \leq 0.9$ g. Employing scaled ground motion would populate the higher range of response, but this would be at the expense of introducing issues of scaling bias. Therefore, unscaled motions have been chosen in this work.

The results are treated using cloud analysis (Cornell et al. 2002). The u_{max} versus PGA data cloud are shown in Fig. 9 left, and they are connected by using linear regression in the logarithmic space: $u_{max} = a \cdot PGA^b$, or by applying logarithms: $\text{Ln}[u_{max}] = \text{Ln}[a] + b \cdot \text{Ln}[PGA]$. The constants are calculated for each particular system (i.e. C_y and u_y are given), see Fig. 9 on the right for the case that is shown here, for which $\text{Ln}[a] = -2.12$ and $b=0.92$, with 0.6 as the standard deviation, σ .

The regression analysis provides the mean and the standard deviation for each value of PGA . In this sample, $\mu = -2.12 + 0.92 \cdot \text{Ln}[PGA]$ and $\sigma = 0.6$. Assuming that $\text{Ln}[u_{max}]$ follows a normal distribution, then u_{max} follows a lognormal distribution, see Fig. 9 on the right. Note that the lognormal distribution characterizes variables with a tendency to produce frequent extremely high values, and it is often used in earthquake engineering, especially when modelling seismic demand.

The lognormal cumulative distribution function gives the probability of occurrence of a given displacement threshold, for example δ , for given values of PGA , C_y , and u_y : i.e. $P[u_{max} \leq \delta \mid PGA, C_y, u_y]$. Figure 10 shows the lognormal cumulative density function for the sample case (i.e., $C_y=0.3$ and $u_y=0.025$ m) and for six different values of PGA .

Finally, considering that $P[u_{max} > \delta \mid PGA_j, C_y, u_y] = 1 - P[u_{max} \leq \delta \mid PGA_j, C_y, u_y]$, the integrand of Eq. (3) is obtained.

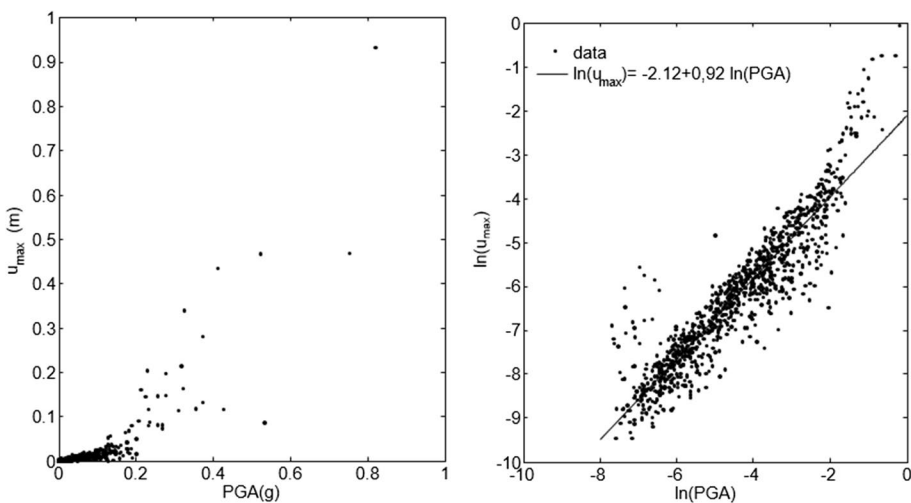
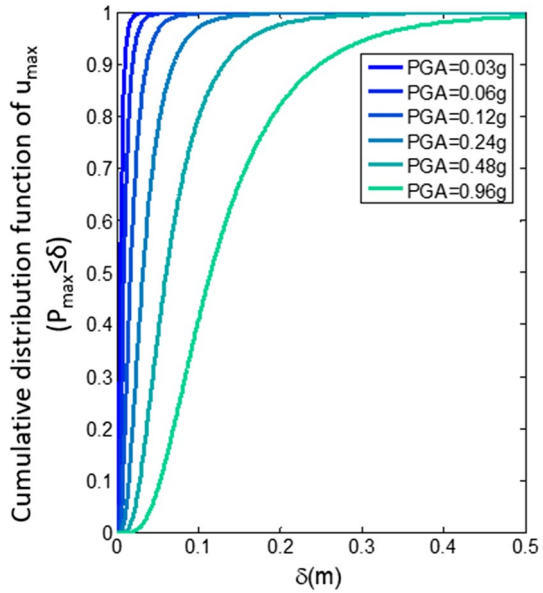


Fig. 9 u_{max} versus PGA (left) and its power-law relationship in logarithmic space (right) for the database of 980 ground motions ($C_y=0.3, u_y=0.025$ m)

Fig. 10 Log Normal Cumulative Distribution Function ($\mu = -2.12 + 0.92 \cdot \ln(\text{PGA})$, $\sigma = 0.6$) for $u_y = 0.025$ m, $C_y = 0.3$, and different values of PGA



The λ - δ curve (see Fig. 6a) is numerically obtained by applying Eq. (4). The seismic hazard curve $\lambda(\text{PGA})$ used in Eq. (4) is the one shown in Fig. 4 (i.e., for the case of Granada).

The displacements (u_{max} and δ) are divided by the yield displacement (u_y), which obtains the ductility demand and the ductility threshold (i.e., a threshold limit in terms of ductility, also called ductility capacity), respectively. Figure 11 shows curve λ - μ (i.e. the YFS) for the sample system ($u_y = 0.025$ m and $C_y = 0.3$) and the location in Granada.

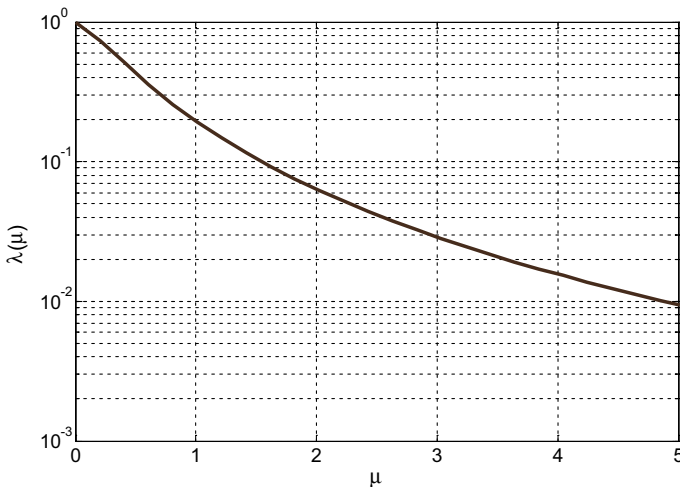


Fig. 11 YFS for $u_y = 0.025$ m, $C_y = 0.3$, and the location in Granada

The above methodology is applied for different SDOF systems after the selection of values of C_y (0.1, 0.2, 0.3, 0.4, 0.5, 0.6, 0.7, 0.8, 0.9, 1) and u_y (0.01 m, 0.025 m, 0.05 m, 0.075 m, 0.1 m). The values of u_{max} versus the *PGA* that are obtained are represented in Fig. 12, and the Yield Displacement Chart for the city of Granada is originally shown in Fig. 13a. Three YFS corresponding to $u_y=0.01, 0.05$ and 0.1 m are displayed in Figs. 13b, c and d to facilitate the interpretation of the Yield Displacement Chart.

7 Example of the design approach

In order to illustrate a design case with multiple performance objectives based on YDC, a simple example has been developed following the flow chart shown in Fig. 14.

The example is a single-column pier of a highway bridge located in Granada (Spain), see Fig. 15. In accordance with (EN1998-1 2004), the design has to fulfill the following two performance objectives:

1. Life safety (LS) requirement, associated with a probability of exceedance of 10% in 50 years (return period of 475 years), i.e. $\lambda_{LS} = -\ln(1-0.1)/50 = 2.11 \times 10^{-3} \text{ years}^{-1}$.
2. Damage limitation (DL) requirement, associated with a probability of exceedance of 10% in 10 years (return period of 95 years), i.e., $\lambda_{DL} = 0.0105 \text{ years}^{-1}$.

The effective yield curvature (ϕ_y) for circular column cross-sections is estimated (Hernández-Montes and Aschheim 2003) as:

$$\phi_y = 2.3 \frac{\epsilon_y}{d} \tag{6}$$

where ϵ_y is the yield strain of the reinforcing steel and d is the depth of the extreme tension reinforcing bar. The characteristic strength of B-400 steel is $f_{yk}=400$ MPa, leading to $\epsilon_y=400/E_s=0.0020$ ($E_s=200,000$ MPa). The column has a circular cross-section with a diameter of 1.2 m. The cover chosen is 2.5 cm, thus $d=1.2-0.05=1.15$ m. The above assumptions results in an effective yield curvature of $\phi_y=0.00397$ rad/m. If overstrength were considered, the value of ϕ_y would be increased (using pushover analysis or code recommendations).

The yield displacement (u_y) for a cantilever column subjected to a lateral load when shear deformation is neglected can be deduced by integrating the curvature along the length of the column twice with $\phi=\phi_y$ for $x=0$, see Fig. 16 and Eq. 7.

$$\phi(x) = \phi_y \frac{L-x}{L} \rightarrow u_y = \int \left(\int \phi(x) dx \right) dx = \phi_y \left(\frac{x^2}{2} - \frac{x^3}{6L} \right) \Big|_0^L = \phi_y \frac{L^2}{3} = 0.048 \text{ m} \tag{7}$$

The DL drift ratio, assumed to be of 2% (EN1998-1 2004), results in a displacement of $0.02 \cdot 6.00 \text{ m} = 0.12 \text{ m}$, and the ductility associated with this displacement is $\mu=0.12/0.048=2.5$.

The target ductility for LS has been chosen following (Mander 1983). According to Figs. 7.10 and 7.11 of (Mander 1983), the ductility capacity goes from 3.0 to 10.0, depending on the confinement and the longitudinal steel ratio. A value of 5.0 has been adopted here for the preliminary design.

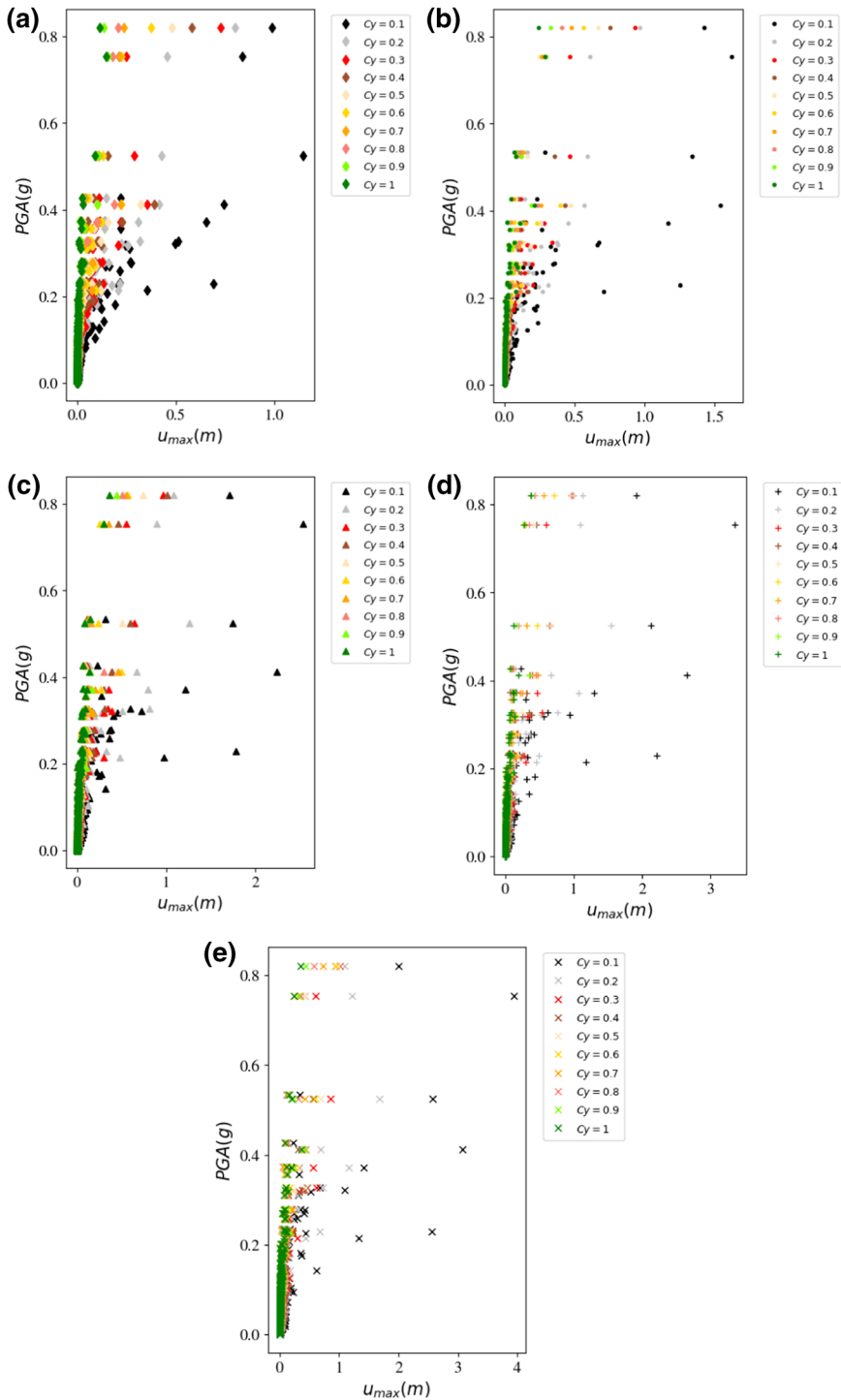
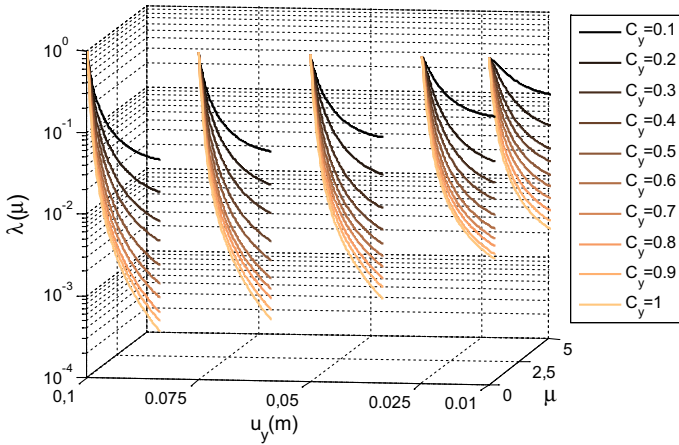
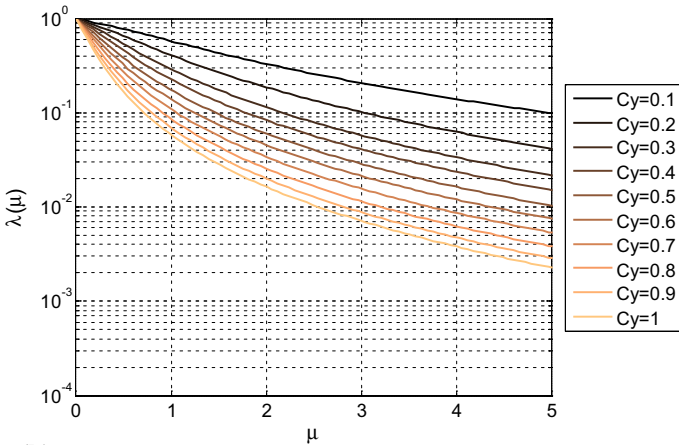


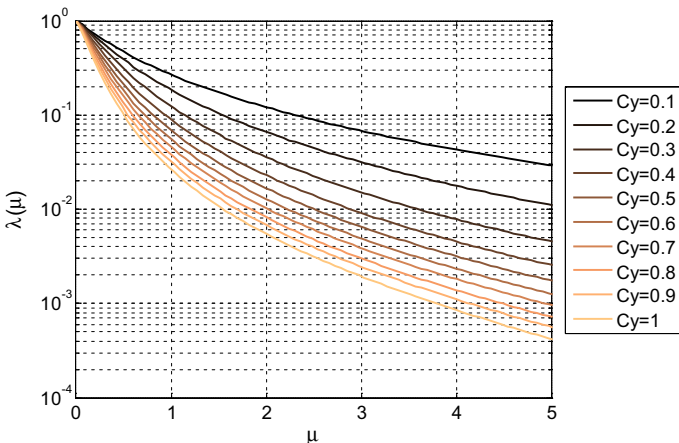
Fig. 12 u_{max} versus PGA. **a** $u_y=0.01$ m, **b** $u_y=0.025$ m, **c** $u_y=0.05$ m, **d** $u_y=0.075$ m, **e** $u_y=0.1$ m. $C_y=(0.1:0.1:1)$



(a) Yield Displacement Chart for the city of Granada.



(b) λ - μ section for $u_y=0.01$ m



(c) λ - μ section for $u_y=0.05$ m

Fig. 13 a Yield displacement chart for the city of Granada. b λ - μ section for $u_y=0.01$ m. c λ - μ section for $u_y=0.05$ m. e λ - μ section for $u_y=0.1$ m

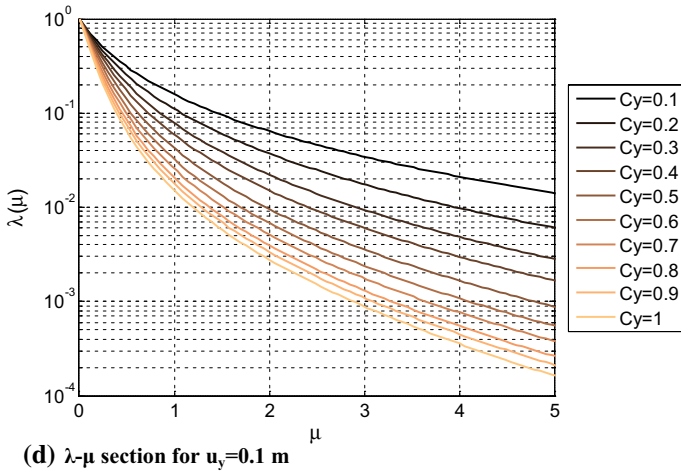


Fig. 13 (continued)

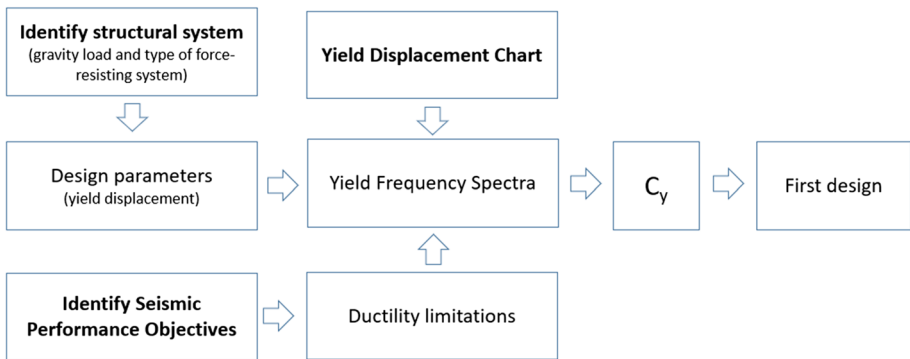


Fig. 14 Flowchart of the design approach

Fig. 15 Bridge column and single-degree-of-freedom model

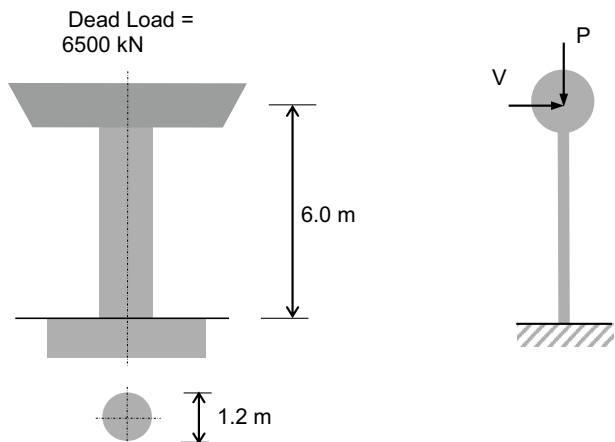
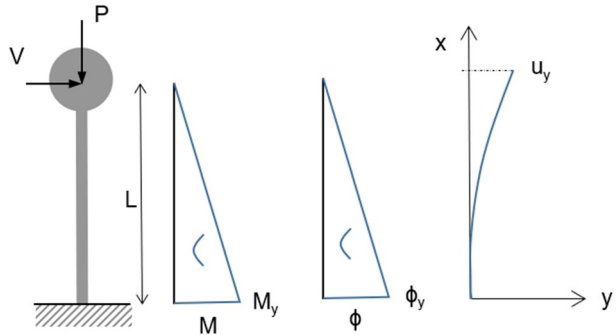


Fig. 16 Yield displacement of a cantilever beam



The YFS for $u_y=0.048$ m (see Eq. 7) is calculated by the linear interpolation between $u_y=0.025$ m and $u_y=0.05$ m in the Yield Displacement Chart (Fig. 13). This YFS and the two performance objectives are represented in Fig. 17. Both performance objectives are expressed in terms of target MAF and ductility: a ductility of 2.5 associated with a MAF of $0.0105 \text{ years}^{-1}$ (which, from Fig. 17, leads to $C_y=0.51$) and a ductility of 5.0 associated with a MAF of $2.11 \times 10^{-3} \text{ years}^{-1}$ (for which $C_y=0.49$). The highest value of C_y is the design value, which in this case is governed by the first performance objective.

So, as the pier is subjected to a dead load of 6500 kN (see Fig. 15), the column has to be designed for a lateral seismic load of $0.51 \cdot 6500 \text{ kN} = 3315 \text{ kN}$.

8 Conclusions

The Yield Displacement Chart tool has been introduced. YDC, as with Yield Point Spectra, are based on the fact that yield displacement remains constant with changes in stiffness, at both sectional and structural levels, thus using the yield displacement of a structure as the design parameter. YDC, like Yield Frequency Spectra, are based on the probability of exceedance of certain performance objectives of equivalent single degree-of-freedom

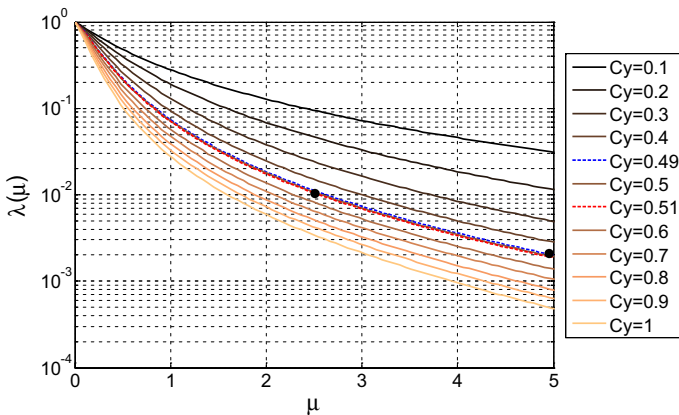


Fig. 17 YFS for $u_y=0.048$ m and the two performance objectives

systems. The novel aspect of YDC is that they consider yield displacement as a variable, so the result is a performance-based seismic design tool that only depends on the geographical location of a structure. YDC must be created in an ad hoc manner for a given site, which means that engineers can use the same Yield Displacement Chart for the same place. YDC are a unique tool for performance-based design.

PGA has been used as intensity measure in the presentation of this new tool (YDC), to emphasize that YDC use the yield displacement as preliminary design parameter, instead of the period. Other intensity measures may give more accurate results, as $S_a(T)$. More research is needed, and conservativeness may be added, e.g. trying several different SDOFs, assessing their MAF via PGA and then via $S_a(T)$, and introducing safety factors based on the obtained differences.

Acknowledgements This work is part of the HYPERION project (<https://www.hyperion-project.eu/>). HYPERION has received funding from the European Union's Framework Programme for Research and Innovation (Horizon 2020) under Grant Agreement No. 821054. The content of this publication is the sole responsibility of the authors and does not necessarily reflect the opinion of the European Union. The authors would like to thank Prof. Dimitrios Vamvatsikos from the National Technical University of Athens for his valuable opinion during the development of his article.

Funding Funding for open access charge: Universidad de Granada / CBUA.

Declarations

Conflict of interest The authors declare that there is no conflict of interest.

Open Access This article is licensed under a Creative Commons Attribution 4.0 International License, which permits use, sharing, adaptation, distribution and reproduction in any medium or format, as long as you give appropriate credit to the original author(s) and the source, provide a link to the Creative Commons licence, and indicate if changes were made. The images or other third party material in this article are included in the article's Creative Commons licence, unless indicated otherwise in a credit line to the material. If material is not included in the article's Creative Commons licence and your intended use is not permitted by statutory regulation or exceeds the permitted use, you will need to obtain permission directly from the copyright holder. To view a copy of this licence, visit <http://creativecommons.org/licenses/by/4.0/>.

References

- ASCE/SEI (2022) ASCE 7 Minimum design loads and associated criteria for building and other structures
- Aschheim M (2002) Seismic design based on the yield displacement. *Earthq Spectra* 18(4):581–600
- Aschheim M, Black EF (2000) Yield point spectra for seismic design and rehabilitation. *Earthq Spectra* 16(2):317–335. <https://doi.org/10.1193/1.1586115>
- Aschheim M, Montes EH (2003) The representation of P- Δ effects using yield point spectra. *Eng Struct* 25(11):1387–1396. [https://doi.org/10.1016/S0141-0296\(03\)00106-8](https://doi.org/10.1016/S0141-0296(03)00106-8)
- Aschheim M, Hernández-Montes E, Vamvatsikos D (2019) Design of reinforced concrete buildings for seismic performance: practical deterministic and probabilistic approaches. CRC Press. Taylor & Francis. <https://www.crcpress.com/Design-of-Reinforced-Concrete-Buildings-for-Seismic-Performance-Practical/Aschheim-Hernandez-Montes-Vamvatsikos/p/book/9780415778817>
- Baker JW (2013) “Probabilistic seismic hazard analysis. White paper version 2.0.” Vol. 79. Stanford CA. [https://web.stanford.edu/~bakerjw/Publications/Baker_\(2013\)_Intro_to_PSHA_v2.pdf](https://web.stanford.edu/~bakerjw/Publications/Baker_(2013)_Intro_to_PSHA_v2.pdf)
- Bazzurro P, Allin Cornell C, Shome N, Carballo JE (1998) Three proposals for characterizing MDOF nonlinear seismic response. *J Struct Eng* 124(11):1281–1289. [https://doi.org/10.1061/\(asce\)0733-9445\(1998\)124:11\(1281\)](https://doi.org/10.1061/(asce)0733-9445(1998)124:11(1281))
- Chopra AK (2020) Dynamic of structures. Pearson education limited, India
- Chopra A, Goel R (2001) Direct displacement-based design: use of inelastic vs. elastic design spectra. *Earthq Spectra* 17(1):47–64
- Cornell CA (1968) Engineering seismic risk analysis. *Bull Seismol Soc Am* 58(5):1583–1606

- Cornell CA, Jalayer F, Hamburger RO, Foutch DA (2002) Probabilistic basis for 2000 SAC federal emergency management agency steel moment frame guidelines. *J Struct Eng* 128(4):526–533
- Cornell CA, Krawinkler H (2000) “Progress and Challenges in Seismic Performance Assessment.” <https://apps.peer.berkeley.edu/news/2000spring/performance.html>
- Deierlein G (2004) Overview of a comprehensive framework for earthquake performance assessment
- EFEHR (2021) European facilities for earthquake hazard and risk. <http://www.efehr.org>
- EN1998–3 (2005). Eurocode 8: design of structures for earthquake resistance - Part 3: assessment and retrofitting of buildings. Brussels
- EN1998–1. 2004. Eurocode 8: Design of structures for earthquake resistance -Part 1: general rules, seismic actions and rules for buildings. EN1998–1. Brussels
- FEMA (2005) “Improvement of nonlinear static seismic analysis procedures, FEMA 440.” Washington, DC
- Fib (2012) “Probabilistic performance-based seismic design. Bulletin 68.” Lausanne, CH
- Giardini D, Woessner J, Danciu L (2014) Mapping Europe’s Seismic Hazard. *Eos* 95(29):261–262
- Heresi P, Dávalos H, Miranda E (2018) Ground motion prediction model for the peak inelastic displacement of single-degree-of-freedom bilinear systems. *Earthq Spectra* 34(3):1177–1199. <https://doi.org/10.1193/061517EQS118M>
- Hernández-Montes E, Aschheim MA (2019) A seismic design procedure for moment-frame structures. *J Earthq Eng* 23(9):1584–1603. <https://doi.org/10.1080/13632469.2017.1387196>
- Hernández-Montes E, Aschheim M (2003) Estimates of the yield curvature for design of reinforced concrete columns. *Magaz Concr Res* 55(4):373–383. <https://doi.org/10.1680/macrc.2003.55.4.373>
- Hernández-Montes E, Chatzidakis A, Gil-Martin LM, Aschheim M, Vamvatsikos D (2019) A seismic design procedure for different performance objectives for post-tensioned walls. *J Earthquake Eng*. <https://doi.org/10.1080/13632469.2019.1691678>
- Kazantzi AK, Vamvatsikos D (2015) Intensity measure selection for vulnerability studies of building classes. *Earthquake Eng Struct Dynam* 44(15):2677–2694. <https://doi.org/10.1002/eqe.2603>
- Luco N, Allin Cornell C (2007) Structure-specific scalar intensity measures for near-source and ordinary earthquake ground motions. *Earthq Spectra* 23(2):357–392. <https://doi.org/10.1193/1.2723158>
- Luco N, Bazzurro P (2007) Does amplitude scaling of ground motion records result in biased nonlinear structural drift responses? *Earthq Eng Struct Dynam* 36:1813–1835. <https://doi.org/10.1002/eqe.695>
- Mander JB (1983) “Seismic design of bridge piers. PhD Thesis.” University of Canterbury. https://www.researchgate.net/publication/34205859_Seismic_design_of_bridge_piers
- Miranda E, Bertero VV (1994) Evaluation of strength reduction factors for earthquake resistant design. *Earthq Spectra* 10(2):357–379
- Nielsen NN, Imbeault FA (1970) “Validity of various hysteresis systems.” In: Proc. of the Third Japan earthquake engineering symposium, 707–14. Tokyo, Japan
- Palermo M, Stefano S, Giada G, Tomaso T (2014) A statistical study on the peak ground parameters and amplification factors for an updated design displacement spectrum and a criterion for the selection of recorded ground motions. *Eng Struct* 76:163–76. <https://doi.org/10.1016/j.engstruct.2014.06.045>
- Palermo M, Silvestri S, Landi L, Gasparini G, Trombetti T (2016) Peak velocities estimation for a direct five-step design procedure of inter-storey viscous dampers. *Bull Earthq Eng* 14(2):599–619. <https://doi.org/10.1007/s10518-015-9829-8>
- Paulay T (2002) A displacement-focused seismic design of mixed building systems. *Earthq Spectra* 18(4):689–718. <https://doi.org/10.1193/1.1517066>
- Priestley MJN (2000) Performance based seismic design. *Bull N Z Soc Earthq Eng* 33(3):325–346
- Priestley MJN, Calvi GM, Kowalsky MJ (2007) Displacement-based seismic design of structures. IUSS Press, Pavia
- Ruiz-García J, Eduardo M (2003) Inelastic displacement ratios for evaluation of existing structures. *Earthq Eng Struct Dyn* 32(8):1237–1258. <https://doi.org/10.1002/eqe.271>
- “RESORCE.” (2020) 2020. www.resorce-portal.eu
- Ruiz-García J, Miranda E (2007) Probabilistic estimation of maximum inelastic displacement demands for performance-based design. *Earthq Eng Struct Dynam* 36(9):1235–1254. <https://doi.org/10.1002/eqe.680>
- SEAOC (1995) “Vision 2000: Performance based seismic engineering of buildings”
- SEAOC (1999) “Recommended lateral force requirements & commentary (Blue Book).” Sacramento, CA
- Vamvatsikos D, Allin Cornell C (2006) Direct estimation of the seismic demand and capacity of oscillators with multi-linear static pushovers through IDA. *Earthq Eng Struct Dynam* 35(9):1097–1117. <https://doi.org/10.1002/eqe.573>
- Vamvatsikos D, Aschheim MA (2016) Performance-based seismic design via yield frequency spectra. *Earthq Eng Struct Dynam* 45:1759–1778

Veletsos AS, Newmark NM (1960) “Effect of inelastic behavior on the response of simple systems to earthquake motions.” In: Proceedings of 2nd world conference on earthquake engineering. Japan

Publisher’s Note Springer Nature remains neutral with regard to jurisdictional claims in published maps and institutional affiliations.